Available online at www.sciencedirect.com

jmr&t Journal of Materials Research and Technology

journal homepage: www.elsevier.com/locate/jmrt

Original Article

Residues from rigid foams and graphene for the synthesis of hybrid polyurethane flexible foams composites

Tamara Calvo-Correas [a,*], Lorena Ugarte [a,b,**], Izaskun Larraza [a], Cristina Peña-Rodríguez [a], M. Angeles Corcuera [a], Arantxa Eceiza [a]

[a] 'Materials + Technologies' Research Group (GMT), Department of Chemical and Environmental Engineering, Faculty of Engineering of Gipuzkoa, University of the Basque Country, Pza Europa 1, Donostia-San Sebastian, 20018, Spain

[b] Department of Graphical Expression and Project Management, Faculty of Engineering of Gipuzkoa, Eibar Section, University of the Basque Country, Otaola Hiribidea 29, Eibar, 20600, Spain

ARTICLE INFO

Article history:
Received 8 January 2021
Accepted 8 April 2021
Available online 15 April 2021

Keywords:
Mechanical recycling
Polyurethane wastes
Graphene residue
Graphite
Hybrid flexible foam composites
Biobased polyol

ABSTRACT

Hybrid biobased polyurethane flexible foam composites containing a residue from surf industry (polyurethane powder) as filler and graphite or graphene residue were synthesized. It was observed that the addition of the powder at low contents did not modify the final properties considerably, since the cell structure was not compromised. Moreover, the powder increased the capacity of the foams to retain the carbonaceous fillers. The compressive properties of the hybrid foams were not altered with the addition of the graphite and graphene. Finally, hybrid composites showed selective absorption capacity since the presence of the carbonaceous fillers provided the foams oil absorption capacity without modifying the hydrophobic nature of the matrix foams.

1. Introduction

The hardening of the legislation on the use and production of plastics has boosted the interest on reducing polymers wastes and on the development of new polymers derived from recycled polymers. Due to the versatility of polyurethanes (PUs), these polymers are placed in fifth among the most produced polymers in Europe and seventh worldwide [1]. In fact, the global production of PU materials in 2017 was 16.9 million tons and it is forecast to increase to 21.3 million tons in 2022 [2], due to the big interest in these materials. PUs are mostly consumed as foams, the 31% of the production are flexible foams, the 25% rigid foams and the 11% are molded foams [3]. Therefore, the production of wastes of these polymeric materials is huge. One of the producers of rigid foams is the surf

* Corresponding author.
** Corresponding author.
E-mail addresses: tamara.calvo@ehu.eus (T. Calvo-Correas), lorena.ugarte@ehu.eus (L. Ugarte).
https://doi.org/10.1016/j.jmrt.2021.04.022

industry. Surf boards are usually made of polyurethane or expanded polystyrene. Nowadays, the global consumption per year of surfboards is over 400,000 and during the shaping process of each board around 0.5 kg of powder waste is produced. In this context, and taking into account that most of the wastes are landfilled, the interest to find a recycling route for them is huge. For example, the initiative created between Surf Industry Manufacturers Association (Sima) and Spillinex™ looks for the reuse of polyurethane dust as absorbent material for oil splits [4].

According to wastes treatment processes, recycling techniques can be classified as primary, secondary, tertiary and quaternary. Primary and secondary recycling or mechanical recycling is based on the reuse of the waste into another product without losing its properties. To that end, techniques such as regrinding [5], rebonding [6], adhesive pressing [7], compression molding [8] or injection molding can be employed [9]. Whereas, in tertiary recycling (chemical recycling) wastes are depolymerized in order to obtain different monomers for their further re-polymerization to regenerate a new polymer. For instance, polyurethanes could be glycolyzated to obtain glycolyzated polyols which could be used as precursors for new polyurethanes [10,11]. Finally, recycling methods based on thermo chemical processing and energy recovery are considered quaternary recycling [9]. Among all the recycling methods, mechanical recycling is considered the most economical and ecofriendly one, since chemical reactions or high temperatures are not required [12].

For the synthesis of polyurethane foams (PUF) two reactions take place, blowing and gelling reaction. In blowing reaction an isocyanate is reacted with a blowing agent, being water the most common. This reaction results in the formation of urea functional groups and carbon dioxide, which allows the growth of the foam and the formation of a porous material. Whereas, gelling reaction arises from the reaction of a polyol and an isocyanate resulting on the formation of urethane groups [13]. Nowadays, most of the raw materials used for the synthesis of PUF are derived from fossil sources, which entails environmental, social and economic concerns and therefore makes the scientific community search new alternatives to replace this kind of precursors. One of the most effective way is the use of polyols derived from vegetable oils such as castor [14], soybean [15] and linseed oil [16].

Carbonaceous nanostructures like graphene and its derivatives have attracted considerable attention in the recent years. The expected superior properties such as high tensile strength or high electrical and thermal conductivity [17], among others, have put graphene in the spotlight for many application fields such as high speed electronics, data storage, solar cells or electrochemical sensing [18]. Parallel to the different applications of graphene, many extraction methods have been developed. Graphene production techniques can be separated in two main groups: bottom-up and top-down methods. Liquid exfoliation is one of the most widespread top-down methods to obtain graphene in small flakes, starting from graphite. In fact, graphene in the form of flakes is the most preferred for the preparation of nanocomposites.

One of the main drawbacks of the liquid exfoliation method is the low yield [19]. In fact, in a previous work graphite flakes were subjected to a liquid exfoliation process with N-methyl-2-pyrrolidone for 100 h [20]. Subsequent stepped centrifugation of the exfoliated suspension resulted in size-selected graphene fractions. In the highest-quality fraction (separated at 4000 rpm), few-layer graphene flakes were obtained. However, on the lowest-quality fraction (separated at 500 rpm) considerable amount of carbonaceous material, that could not be considered few-layer graphene, was obtained. This rejected fraction, hereby referred as graphene residue (GR), was considered in the present work as a filler for oil-water separation 3D sponges, providing a suitable material for this application and increasing the yield of the liquid exfoliation method. In fact, in other works both graphene and graphite have been effectively used as fillers in 3D sponges for oil-water separation [21] due to their hydrophobic and oleophilic nature. Apart from graphene, carbon based materials such as multi-walled carbon nanotubes [22–24], activated carbon [25] or carbonaceous nanoparticles [26] have been satisfactorily incorporated in foam formulation in order to increase oleophilicity. However, no works concerning the incorporation of recycled carbonaceous nanoparticles were reported. In addition, the most common method for the addition of carbonaceous nanoentities is the *in-situ* incorporation. Compared to *in-situ* incorporation method, the impregnation of foams with the nanoentities shows several advantages. On the one hand, it offers the possibility of impregnating waste foams, contributing to the reuse of residues. On the other hand, *in-situ* incorporation of nanoparticles could modify viscosity and hence the reaction kinetics of foams and formulations should be readjusted for each nanoparticle content [14]. Moreover, high nanoparticle contents, could lead to foam collapse.

Therefore, the main objective of this research is to develop hybrid biobased polyurethane foams composites containing different amounts of recycled polyurethane powder and graphite or GR. Carbonaceous nanoentitites were incorporated by impregnation method due to its advantages. The used recycled fillers were characterized using different microscopy and spectroscopy techniques. Moreover, the dynamic mechanical, thermogravimetric and mechanical properties of the developed foam composites were analyzed. Finally, oil absorption capacity of the foams was also evaluated.

2. Experimental section

2.1. *Materials*

B-side of the formulation is constituted by a castor oil derived polyol (Lupranol 2005/1/balance from BASF, with a hydroxyl number of 50.31 mgKOH g^{-1}, determined according to ASTM D4274-05 standard, and a biobased carbon content of 35%, determined according to the procedure of ASTM-D6866-12 (0.98) Method B (AMS) standard), distilled water as blowing agent, two catalysts (Tegoamin® B75 (amine catalyst) and Kosmos®29 (tin catalyst)) and a surfactant (Tegostab® B-4900), all of them from Evonik. Whereas the A-side was formed by toluene diisocyanate (TDI), which was kindly supplied by Covestro. As fillers polyurethane rigid foam powder (PUP), residue resultant from surf industry, kindly supplied by Olatu

S.A., graphite (G) from Aldrich and graphene residue (GR), resultant from the exfoliation of graphite in N-methyl pyrrolidone for the obtaining of graphene, were used. Sodium dodecyl sulphate (SDS) (96%) from Fluka was used as surfactant to allow the dispersion of graphite and GR in water.

2.2. Synthesis of flexible foam composites with recycled PU powder

Foams were prepared following a two-step reaction procedure. To that end, the B-side (polyol, water, catalysts and surfactant) was vigorously mixed during 2 min at 2000 rpm. Subsequently, the A-side (TDI) was added and it was mixed for 7 s at the same speed rate. After that, the resultant mixture was poured into an open mold to freely rise the foam. Foams were cured at room temperature (RT) during 24 h. After that, foams were post cured in an oven at 150 °C for 24 h to complete the reaction of isocyanate groups. In the case of the composites with PUP, it was added to the polyol and stirred at 1000 rpm until a homogeneous mixture was obtained. The flask containing the mixture during the stirring was kept into iced-water to avoid the increase of the temperature. After that, foams were prepared following the previously described procedure. Foams containing from 0 to 20% of PUP were prepared, according to the formulation described in the Supporting Information (Table S1). Samples were designed as PUFx, being x de percentage of PUP.

2.3. Preparation of hybrid foam composites with graphite and graphene residue

First of all, graphite or GR were mixed with a surfactant (SDS) and distilled water (1 mg filler/0.5 mg SDS/1 mL water). In the case of graphite dispersion, it was ultrasonicated with an amplitude of 30% for 1.5 h, while GR was dispersed in a sonication bath with iced water for 30 min. After that, each foam was impregnated with 12 mL of dispersion by forcing the dispersion to pass through the pores of the foams 9 consecutive times (Fig. 1a). After impregnation foams were placed in a vacuum oven at 45 °C at 55 mbar for 4 days. The resultant foams are shown in Fig. 1b. Foams have been coded as PUFx-y, where x is the amount of PUP and y is ascribed to the impregnated carbonaceous filler i.e. G or GR.

2.4. Characterization techniques

Fourier transform infrared spectroscopy (FTIR) was used in order to determine the characteristic bands and the purity of the recyclable PUP. To that end, the accessory MKII Golden Gate Attenuated Total Reflection was equipped to a Nicolet Nexus FTIR spectrometer, with lens of ZnSe and a diamond crystal at an angle of 45°. The spectrum was obtained after 32 scans at a resolution of 4 cm^{-1} at a wavenumber from 4000 to 650 cm^{-1}.

A JSM-6400 scanning microscope was used to study the morphology of the prepared foams with PUP. The operating distance was 7 mm and the voltage 20 kV. A coating of gold of 20 nm (Quorum Q150TES) was applied to foams to make them conductors.

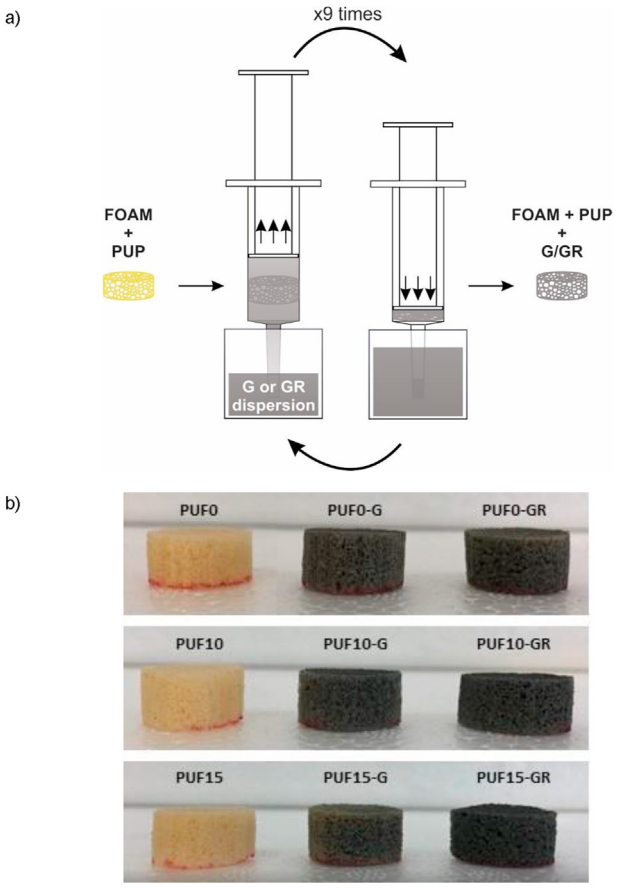

Fig. 1 – a) Scheme of the impregnation procedure of foams with G and GR and b) digital images of the prepared hybrid foam composites with G and GR.

The ratio between weight and volume of the prepared foam composites was used to calculate their density. Density values of at least three specimens were used to average the values.

A CellFlo foam porosity meter (IDM instruments) was used for the determination of the open cell content of the prepared foams with PUP and hybrid composite foams. To that end, an air flow parallel to grow direction was passed through the cellular structure of the foam at RT.

The dynamic mechanical properties of the prepared foams with PUP were studied by dynamic mechanical analysis (DMA) in compression mode using an Eplexor 100 N analyzer (Gabo). Measurements were carried out from −100 to 250 °C at scanning rate of 2 °C min^{-1}, at a frequency of 1 Hz and a static strain of 0.3%. Samples were cut in square shape with a side of 17 mm and height of 12 mm.

Thermogravimetric analysis (TGA) was used to determine the amount of GR and graphite impregnated in foams, using a Mettler Toledo TGA/SDTA851 analyzer. A heating scan from 25 to 800 °C at a heating rate of 10 °C min^{-1} was performed under nitrogen atmosphere and the residue was measured. The carbonaceous filler amount was determined according to Eq. (1):

$$Filler\ amount\ (\%) = R_{hybrid} - R_{reference} \quad (1)$$

a)


PUF0
PUF10
PUF15
PUF20

b)

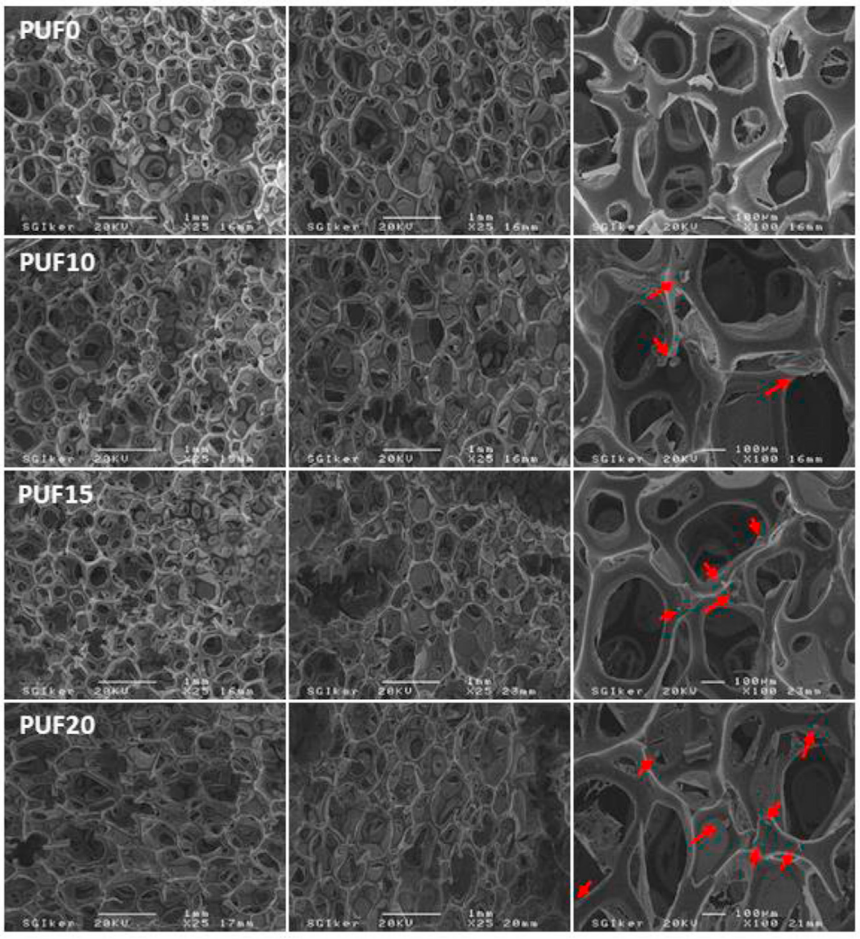
PUF0
PUF10
PUF15
PUF20

c)

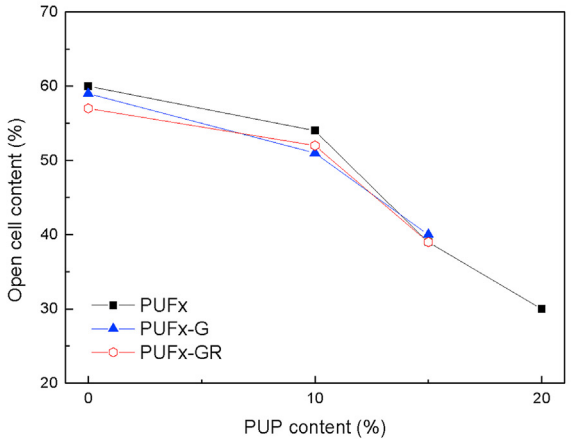
Open cell content (%)
PUP content (%)
PUFx
PUFx-G
PUFx-GR
70
60
50
40
30
20
0
10
20

where R_{hybrid} is the residue of the hybrid foam composite and $R_{reference}$ is the residue of the foam composite with PUP.

Raman spectra of GR and graphite were obtained with a Renishaw InVia microscope (50×) with a laser of 514 nm wavelength (Modu Laser) at a potency of 10%. Data were collected in the range of 150–3500 cm^{-1}. Exposure time and accumulations were set at 20 s and 5 s, respectively.

Atomic force microscopy (AFM) analysis was carried out to observe the size of GR. Height images were obtained in a Dimension Icon scanning probe microscope equipped with Nanoscope V controller (Bruker). Tapping mode was employed in air using an integrated tip/cantilever (125 μm length with ca. 300 kHz resonant frequency). For sample preparation, GR fraction was dispersed in cyclohexane (CH) (0.0025 mg mL^{-1}) using an ultrasonic tip for 1 h. To avoid solvent evaporation, a pulsed sonication program was applied, with ON/OFF periods of 4 and 2 s, respectively. A droplet of GR suspension was put on a prewashed silicon wafer substrate and dried at RT for 48 h.

Compressive properties of the prepared composite foams were carried out at RT in a Universal testing machine (Instron 5967) equipped with 10 kN load cell at a crosshead speed of 50 mm min^{-1}. Square shape samples (side 50 mm x height 30 mm) were compressed at 80% of the height of the foam. According to ASTM D 1621-16 standard [27], compressive strength (σ_c) was taken as the stress in the yield point, compression modulus (E_c) is the slope in the elastic region of the stress–strain curve and densification strain (ε_d), calculated as the strain in the intersection point between the stress plateau and the densification slope. Results were averaged from four measurements.

In order to determine the absorption capacity at RT (Q) of the prepared foams composites, cylindrical shape samples were cut with a diameter of 10 mm and height of 20 mm. Samples were immersed in pump oil for 1 and 90 min. Foams were weighted before and after each immersion. Absorption capacity was calculated according to Eq. (2):

$$Q = \frac{w_w}{w_0} \quad (2)$$

where w_w is the weight of the sample after immersion and w_0 is the initial weight.

3. Results and discussion

First of all, since the rise and the final properties of foams composites are closely dependent to the amount and size of the added filler, the employed PUP was characterized in the macro and micro scale. At first sight, it is observed that PUP is heterogeneous and contained small splinters from the stringer, which is made of wood. Therefore, biggest splinters were removed and the resultant fraction was grinded in a mill equipment with a sieve of 500 μm to homogenize the PUP. In this way, the amount of PUP in PUF formulation can be increased. The size distribution of the grinded homogenous powder is 225 ± 45 μm (Fig. S1a and b). Furthermore, it was determined that 75% of the residue can be recycled for foam formulation. Besides, the grinder PUP was characterized by FTIR, observing the characteristic spectrum of a polyurethane (Fig. S1c), denoting that the amount of splinters that could be grinder during homogenization process is minimum and PUP is principally constituted by polyurethane.

Due to density of the foams being of utmost importance, since it determines the compressive properties of foams [28], the density of the prepared composites was determined. Density of foams is strongly dependent on the mass and the viscosity of the expandable polymer and, hence, on the amount of blowing agent, which in this work was kept constant. Furthermore, it can also be modified with the addition of fillers, since they could interfere in the nucleation step of the foam. Filler addition could hinder the rise of the foams, leading to a higher solid phase instead of gaseous, increasing foams' density [29,30]. The addition of PUP lead to the obtaining of denser foams, since the obtained values are 37.4, 47.2, 49.7 and 51.2 kg/m^3 for PUF0, PUF10, PUF15 and PUF20, respectively. Furthermore, the effect of the addition of PUP on the rise of the foams is notorious (Fig. 2a). The volume of foams decreases as PUP content increases, which could be attributed to the observed higher viscosity of the mixture formed by the polyol and PUP [31].

The final properties of foams are also strongly influenced by their cellular structure. Therefore, their morphology was studied by SEM. In Fig. 2b SEM micrographs of the foam composites are shown. All the synthesized composites show polyhedral open and closed cells. As mentioned before the viscosity of the mixture formed by the polyol and PUP increases with PUP content. This increase could interfere in the cellular structure of the foam, favoring the formation of a more heterogeneous structure [32]. In the case of PUF10, cell structure is similar to PUF0, denoting that the addition of PUP up to this content does not interfere in it to a great extent. However, when higher amount of PUP is incorporated, cells are more damaged, especially in PUF20. This fact could be attributed to both the aforementioned higher viscosity of the mixture and the higher amount of PUP embedded in the struts. The embedded PUP, indicated with arrows in the magnification of Fig. 2b right, can act as cells' breaking points [14]. Moreover, foam composites show good adhesion between PUP and struts, since there are hardly any signs indicating that the filler has come out the struts, such as holes.

Furthermore, the open cell content of the prepared foams with PUP was determined (Fig. 2c). As can be seen, as PUP content increases foams show a lower open cell content. Cell opening depends on different factors, such as viscosity, isocyanate index, the nature of the surfactant, the amount of the catalyst and the presence of fillers [33]. Therefore, the lower content of open cells could be attributed to the mentioned

Fig. 2 – Characterization of synthesized foams composites with different content of PUP: a) Digital images of the prepared PUF composites before post-curing process, b) SEM micrographs taken parallel to foams growth (left), perpendicular to foams growth (center) and magnification of the section in the perpendicular plane (arrows indicate PUP) (right) and c) open cell content of the prepared foams.

higher viscosity of the mixture because of the higher amount of PUP [34] that hindered wall breakage [33].

The dynamic mechanical properties of the PUF composites were analyzed by DMA (Fig. 3). All PUF show an α transition temperature (T_α) at low temperatures, almost independent to PUP content (−48.1, −44.8, −45.5 and −43.6 °C for PUF0, PUF10, PUF15 and PUF20, respectively), denoting that prepared foams are flexible, in accordance to the open cell content determined by the porosity meter. The addition of PUP decreases the storage modulus, which could be related with the morphology of the foams. As previously observed, as PUP content increases cells were more damaged, especially in PUF20, since PUP particles go through them deteriorating their structure [35]. This deterioration resulted in materials with lower stiffness. Furthermore, the prepared foam composites show a high thermal stability since foams do not collapse before 220 °C.

In sight of the observed results, since the addition of PUP at high contents damages the cellular structure and, hence, worsens the final properties of foam composites, it was decided not to use PUF20 foam to obtain hybrid foam composites. During impregnation process, G and GR are adhered to cells struts, thus, broken cells would not be optimum for the impregnation process. That is why, only PUF10 and PUF15 were impregnated with G and GR, as well as PUF0, as reference, in order to determine if the presence of the recyclable PUP could contribute to the impregnation of the carbonaceous fillers.

First of all, GR and G were characterized by Raman spectroscopy to analyze their structure. As can be observed in Fig. 4a, both GR and graphite show typical carbon materials spectra with peaks corresponding to G (1580 cm^{-1}), D (1350 cm^{-1}) and 2D (2700 cm^{-1}) bands. G band is related to the in-plane vibration mode caused by the stretching of sp^2 carbon pairs, while 2D band is associated with the second order of zone boundary phonons [36]. In few-layer graphene, the shoulder observed in the 2D band disappears, becoming a unique sharp peak [37,38]. In this case, the shoulder is observed in both GR and graphite suggesting that GR is composed by multiple graphene layers. D band can be taken as an indicative of flake edges, since it is related to defects in the carbon structure [38,39]. The increase in D band intensity in GR may denote an increase of flake edges in GR as a consequence of the exfoliation process. Moreover, the I_D/I_G ratio can be directly related to the in-plane flake size [39–41]. 0.06 and 0.14 values are calculated for G and GR, respectively, suggesting a decrease in flake size in GR due to exfoliation.

Furthermore, flake size and thickness of GR was analyzed by AFM. Height images and their corresponding cross sectional profiles, calculated along the indicated lines, are shown in Fig. 4b. On the images, flakes of around 2 μm are observed as well as some agglomerates corresponding to poorly exfoliated bulk graphite. Cross sectional profiles reveal thickness values around 8 nm. According to literature, monolayer or few-layer graphene thickness values are in the range of 0.35–1.5 nm when determined by AFM [42,43]. In consequence, GR flakes might correspond to multilayer graphene or nanographite.

Results concerning the filler content of hybrid composite foams after impregnation are shown in Table 1. Similar values

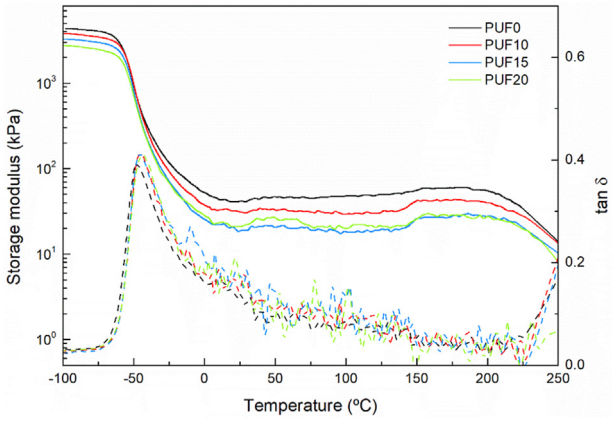

Fig. 3 – Evolution of storage modulus (solid line) and tan δ (dash line) with temperature of foams with different contents of PUP.

were determined by both weight difference and by TGA techniques (see supporting information S2). The impregnation efficiency of the foams was also calculated taking into account the initial filler content in the dispersion and the final amount in the impregnated foams. It was observed that it is around 60% for foams with G and 40% for the ones with GR. It can be observed that for each foam, G amount is higher than GR amount. That could be related to the bigger size of non-exfoliated G flakes that are more easily retained in the foam structure. When comparing the effect of PUP, it is spotted that the highest filler content is obtained for PUF10 series, while it is quite similar for both PUF0 and PUF15 series. That might be a consequence of the effect of PUP in the foam structure. As observed previously in Fig. 2c, in PUF10 sample the amount of closed cells increases as a consequence of the increase of reacting mixture viscosity. As a result, the retained G and GR amount increases in PUF10 series. However, in PUP15 series, the damage in cell walls could compensate the increase of closed cell content, obtaining similar filler contents to PUF0 series. Furthermore, it was observed that neither the addition of G and GR nor the employed addition method modified in a great extent the content of open cells, since similar amounts were measured.

Compressive mechanical properties of hybrid composite foams are gathered in Table 2. It can be observed that the incorporation of PUP does not modify the mechanical properties, except in PUF15 series. As aforementioned, the addition of PUP in contents higher than 10 wt% damage the cellular structure of the foams. Therefore, this series do not show the same tendency of PUF0 and PUF10 series. Regarding mechanical properties of PUF0 and PUF10 series, as can be seen yield strength values are not influenced by the incorporation of G and GR. A slight increase of Young's Modulus is observed, suggesting that the presence of both particles increases the stiffness of the foams. These slight increases could be related to the filler content in each foam, since the amount of G is higher in both PUF0-G and PUF10-G foams. In the case of GR, it should be taken into account that the modulus value determined for PUF0-GR show a considerable deviation, if

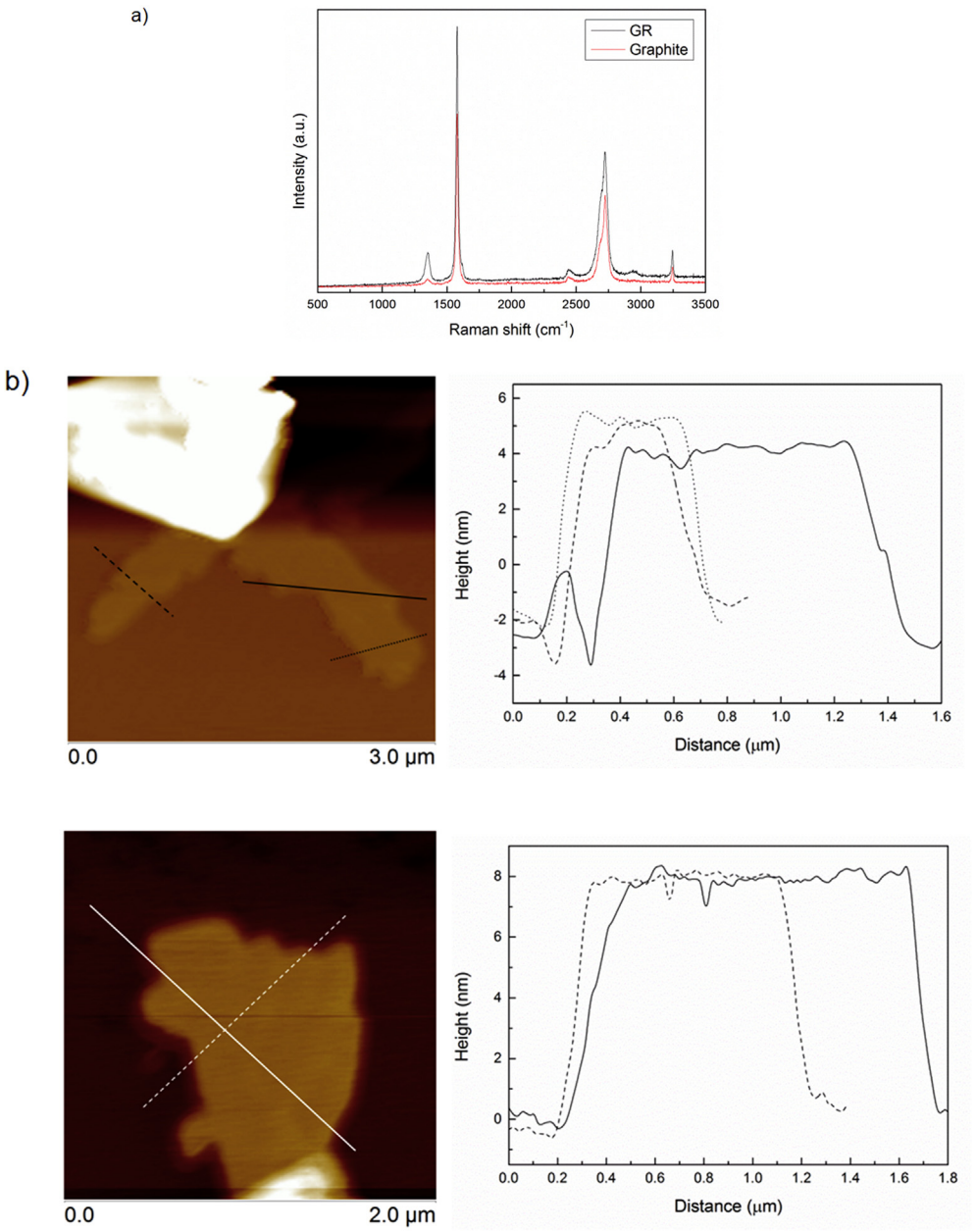

Fig. 4 – Characterization of the carbonaceous fillers: a) Raman spectra of GR and graphite and b) AFM height images (left) and cross sectional profiles (right) of GR obtained in two different regions of the sample.

compared with the deviations calculated for the rest of the series. Considering this fact, it could be said that higher amounts of GR resulted in higher modulus values.

As a general tendency, densification strain values decrease with the incorporation of G and GR. Taking into account that the densification strain represents the beginning of cell wall interactions, the obtained results can be explained by the thickening of cell walls due to the presence of G and GR flakes and the decrease of open cell content. In any case, the observed variations of the properties are not remarkable, hence, it can be said that the hybrid composite foams keep the polymer foam behavior.

The absorption behavior of prepared hybrid composite foams is shown in Fig. 5. All samples show hydrophobic behavior since water drop remains unvaried on the samples surface. Apart from the chemical composition of the polyurethane foam, the rough surface of the foam may be a key factor ruling the hydrophobic behavior [44]. With relation to this, the air trapped in polyurethane foam cells could favor heterogeneous wetting on the hydrophobic surface [45]. In bare PUP samples, oil drop can also be observed on the surface. Although the contact angle is lower than in the case of the water drop, PUP foams do not show oleophilic behavior. On the contrary, when an oil drop is poured on hybrid

Table 1 – Filler content (wt%) of hybrid foam composite samples determined by weight difference and by TGA and oil absorption capacity (Q) of the composite foams determined at 1′ and 90′ of immersion.

Sample	Filler content (wt%) by weight difference	Filler content (wt%) by TGA	Q		Q (mg^{-1} G or GR)	
			1′	90′	1′	90′
PUF0-G	4.70 ± 0.60	3.42	14.0 ± 2.4	19.5 ± 0.1	2.0 ± 0.5	2.7 ± 0.3
PUF0-GR	2.80 ± 0.34	2.98	14.4 ± 2.2	19.6 ± 0.6	3.5 ± 0.5	4.8 ± 0.7
PUF10-G	5.66 ± 0.43	5.73	21.4 ± 1.6	23.4 ± 0.9	2.9 ± 0.1	3.2 ± 0.2
PUF10-GR	3.45 ± 0.14	3.02	19.0 ± 2.6	22.7 ± 1.2	4.0 ± 0.6	4.9 ± 0.3
PUF15-G	3.75 ± 0.80	4.10	10.9 ± 1.7	13.6 ± 1.7	1.6 ± 0.3	2.2 ± 0.5
PUF15-GR	2.74 ± 0.23	2.46	11.0 ± 2.8	13.0 ± 1.1	1.8 ± 0.4	2.2 ± 0.1

Table 2 – Filler content, Yield strength, Young's modulus and densification strain of reference and hybrid (containing G and GR) composite foam series. Normalized values.

	Filler content (wt%) by weight difference	$\sigma_{c\ yield}/\rho$ (kPa m^3/kg)	E_c/ρ (kPa m^3/kg)	Densification strain/ρ (%m^3/kg)
PUF0	–	0.08 ± 0.02	1.74 ± 0.31	1.74 ± 0.08
PUF0-G	4.70 ± 0.60	0.11 ± 0.02	1.94 ± 0.13	1.72 ± 0.13
PUF0-GR	2.80 ± 0.34	0.11 ± 0.02	2.17 ± 0.82	1.62 ± 0.02
PUF10	–	0.09 ± 0.02	1.72 ± 0.38	1.83 ± 0.14
PUF10-G	5.66 ± 0.43	0.10 ± 0.01	2.26 ± 0.13	1.87 ± 0.06
PUF10-GR	3.45 ± 0.14	0.10 ± 0.01	1.76 ± 0.36	1.78 ± 0.05
PUF15	–	0.05 ± 0.03	0.69 ± 0.12	1.34 ± 0.18
PUF15-G	3.75 ± 0.80	0.04 ± 0.03	0.64 ± 0.08	1.37 ± 0.19
PUF15-GR	2.74 ± 0.23	0.06 ± 0.02	0.75 ± 0.22	1.16 ± 0.14

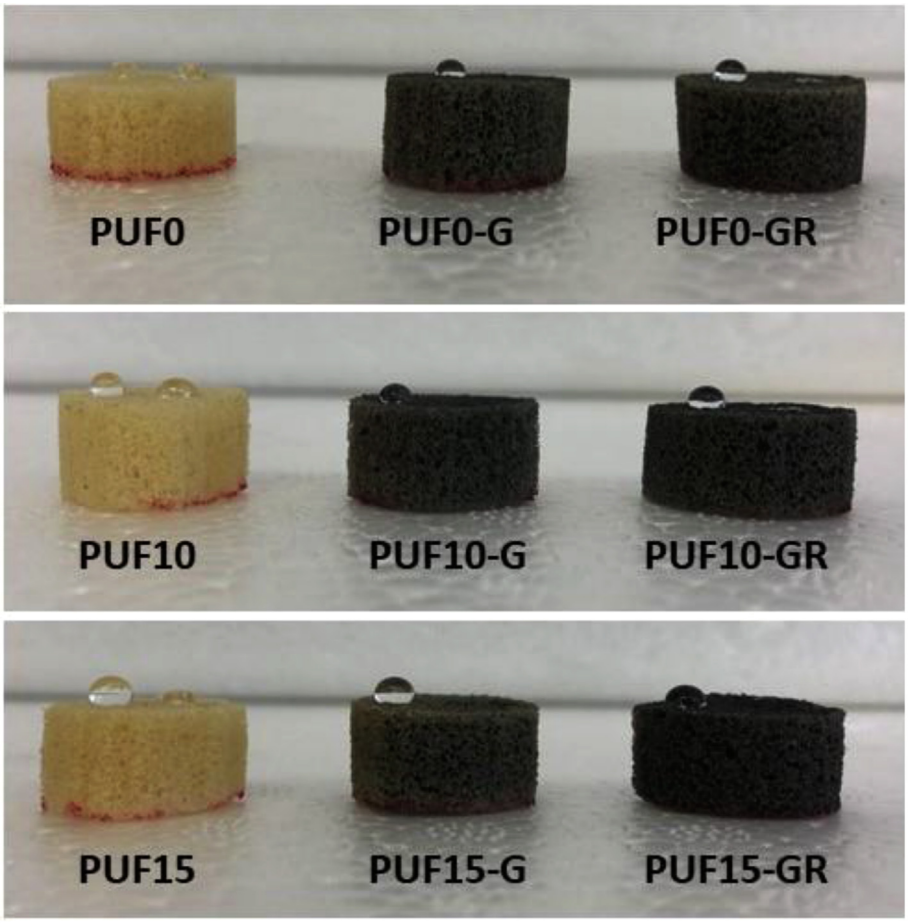

Fig. 5 – Digital images of hybrid composite foam series with drops of water (left) and of oil (right).

composite foams surface, it is immediately absorbed (see available videos in supplementary information) and no oil drop can be observed on the image. Thus, it is confirmed that G and GR presence confers selective oil absorption capacity to the foams.

Supplementary video related to this article can be found at https://doi.org/10.1016/j.jmrt.2021.04.022

In light of the oleophilic behavior observed for the hybrid foams, their absorption capacity was quantified. To that end, foams were immersed into pump oil during different times. In Table 2 the obtained results are gathered. As can be observed, the oil absorption capacity is dependent on the immersion time, since absorption capacity increases with time. PUF10 foams show the highest oil absorption capacity, in accordance to the presence of a higher amount of carbonaceous filler. Moreover, as mentioned before, the addition of carbonaceous fillers did not influence the amount of open cells. This fact denotes that the observed oleophilicity could be ascribed to the presence of the fillers and not to a modification of the cellular structure. On the other hand, the oil absorption capacity per mg of filler reveals that hybrid foams containing GR show a higher capacity, which could be attributed to the higher surface area of the GR. However, since the content of graphite is higher in the foams, their overall absorption is higher.

4. Conclusions

Hybrid polyurethane flexible foam composites containing different amounts of recycled polyurethane powder and impregnated with carbonaceous fillers, i.e. graphite and graphene residue (GR), were successfully prepared. The employed grinding technique of polyurethane powder was a solid way to process the waste, since in that way the 75% of the powder was suitable for foams formulation. Furthermore, it was observed that the addition of polyurethane powder at low contents (10 wt%) did not interfere in cell structure to a great extent and, hence, the properties of the foams were not greatly compromised. The employed GR, obtained as a by-product from graphene exfoliation process, showed an intermediate morphology between few-layer graphene and graphite. Raman and atomic force microscopy results confirmed its carbonaceous nature and multi-layer structure. The presence of the recycled powder at low content increased the ability of the composite foam to retain a higher amount of carbonaceous filler after the immersion. Concerning the mechanical properties, hybrid foams prepared with both graphite and GR kept the flexible behavior of the reference foam and no important rigidization effect was observed. Hybrid composite foams maintained the hydrophobic behavior of the polymeric foam. Furthermore, the presence of graphite and GR conferred oleophilic nature and selective oil absorption capacity. In this way, the spongy characteristics of the hybrid composite foams and their improved oleophilic behavior make them suitable candidates for selective oil water separation materials.

Declaration of Competing Interest

The authors declare that they have no known competing financial interests or personal relationships that could have appeared to influence the work reported in this paper.

Acknowledgments

Authors thank the University of the Basque Country (UPV/EHU) (GIU18/216 Research Group), the Basque Government (PIBA19-0044 project) and the Provincial Country of Gipuzkoa (DG 19/28 Support Program for the Guipuzcoan Science, Technology and Innovation Network 2019) for the financial support. We also acknowledge the "Macrobehavior-Mesostructure-Nanotechnology" SGIker unit from the UPV/EHU, for their technical support and Olatu S.A. (Gipuzkoa) for providing the PUP. T.C-C. thanks the Provincial Country of Gipuzkoa (2017-BE01-000002-01) and the UPV/EHU (ESPDOC19/41).

Appendix A. Supplementary data

Supplementary data to this article can be found online at https://doi.org/10.1016/j.jmrt.2021.04.022.

REFERENCES

[1] Plastics – the Facts 2017. An analysis of European plastics production, demand and waste data, (n.d.). https://www.plasticseurope.org/application/files/5715/1717/4180/Plastics_the_facts_2017_FINAL_for_website_one_page.pdf.
[2] Global polyurethane demand 2012-2022, (n.d.). https://www.statista.com/statistics/747004/polyurethane-demand-worldwide/..
[3] Polyurethane production, pricing and market demand, (n.d.). https://www.plasticsinsight.com/resin-intelligence/resin-prices/polyurethane/..
[4] Staff U. Surfboard brands reuse PU foam dust. 2011. https://www.utech-polyurethane.com/news/surfboard-brands-reuse-pu-foam-dust.
[5] Khoshnoud P, Wolgamott JC, Abu-Zahra N. Evaluating recyclability of fly ash reinforced polyvinyl chloride foams. J Vinyl Addit Technol 2018;24:154–61.
[6] Sims GLA. Recycling of automotive foam/fabric laminates by incorporation into rebounded polyurethane foam. Cell Polym 1996;15:436–49.
[7] Bekhta P, Lyutyy P, Ortynska G. Properties of veneered flat pressed wood plastic composites by one-step process pressing. J Polym Environ 2017;25:1288–95.
[8] Leger E, Landry B, LaPlante G. High flow compression molding for recycling discontinuous long fiber thermoplastic composites. J Compos Mater 2020;23:3343–50.
[9] Zia KM, Bhatti HN, Ahmad Bhatti I. Methods for polyurethane and polyurethane composites, recycling and recovery: a review. React Funct Polym 2007;67:675–92.
[10] Calvo-Correas T, Ugarte L, Trzebiatowska PJ, Sanzberro R, Datta J, Corcuera MÁ, et al. Thermoplastic polyurethanes

with glycolysate intermediates from polyurethane waste recycling. Polym Degrad Stabil 2017;144:411–9.
[11] Datta J. Synthesis and investigation of glycolysates and obtained polyurethane elastomers. J Elastomers Plastics 2010;42:117–27.
[12] Maris J, Bourdon S, Brossard JM, Cauret L, Fontaine L, Montembault V. Mechanical recycling: compatibilization of mixed thermoplastic wastes. Polym Degrad Stabil 2018;147:245–66.
[13] Ashida K. Polyurethane foams in polyurethane and related foams: chemistry and technology. Boca Raton, FL: CRC Press; 2007.
[14] Gómez-Fernández S, Ugarte L, Calvo-Correas T, Peña-Rodríguez C, Corcuera MA, Eceiza A. Properties of flexible polyurethane foams containing isocyanate functionalized kraft lignin. Ind Crop Prod 2017;100:51–64.
[15] Guo A, Javni I, Petrovic Z. Rigid polyurethane foams based on soybean oil. J Appl Polym Sci 2000;77:467–73.
[16] Calvo-Correas T, Mosiewicki MA, Corcuera MA, Eceiza A, Aranguren MI. Linseed oil-based polyurethane rigid foams: synthesis and characterization. J Renew Mater 2015;3:3–13.
[17] Novoselov KS, Fal'Ko VI, Colombo L, Gellert PR, Schwab MG, Kim K. A roadmap for graphene. Nature 2012;490:192–200.
[18] Randviir EP, Brownson DAC, Banks CE. A decade of graphene research: production, applications and outlook. Mater Today 2014;17:426–32.
[19] Buzaglo M, Ruse E, Levy I, Nadiv R, Reuveni G, Shtein M, et al. Top-down, scalable graphene sheets production: it is all about the precipitate. Chem Mater 2017;29:9998–10006.
[20] Ugarte L, Gómez-Fernández S, Tercjak A, Martínez-Amesti A, Corcuera MA, Eceiza A. Strain sensitive conductive polyurethane foam/graphene nanocomposites prepared by impregnation method. Eur Polym J 2017;90:323–33.
[21] Jiang P, Li K, Chen X, Dan R, Yu Y. Magnetic and hydrophobic composite polyurethane sponge for oil-water separation. Appl Sci 2020;10:1453–66.
[22] Ma X, Zhang C, Gnanasekar P, Xiao P, Luo Q, Li S, et al. Mechanically robust, solar-driven, and degradable lignin-based polyurethane adsorbent for efficient crude oil spill remediation. Chem Eng J 2021;415:128956.
[23] He X, Lin S, Feng X, Pan Q. Synthesis and modification of polyurethane foam doped with multi-walled carbon nanotubes for cleaning up spilled oil from water. J Polym Environ 2020. https://doi.org/10.1007/s10924-020-01942-1.
[24] Zhang T, Gu B, Qiu F, Peng X, Yue X, Yang D. Preparation of carbon nanotubes/polyurethane hybrids as a synergistic absorbent for efficient oil/water separation. Fibers Polym 2018;19:2195–202.
[25] Keshavarz A, Zilouei H, Abdolmaleki A, Asadinezhad A, Nikkhah AA. Impregnation of polyurethane foam with activated carbon for enhancing oil removal from water. Int J Environ Sci Technol 2016;13:699–710.
[26] Shi H, Shi D, Yin L, Yang Z, Luan S, Gao J, et al. Ultrasonication assisted preparation of carbonaceous nanoparticles modified polyurethane foam with good conductivity and high oil absorption properties. Nanoscale 2014;6:13748–53.
[27] International Organization for Standardization, ASTM D1621-16. Standard test method for compressive properties of rigid cellular plastics. 2016. p. 1–5.
[28] Thirumal M, Khastgir D, Singha NK, Manjunath BS, Naik YP. Mechanical, morphological and thermal properties of rigid polyurethane Foam: effect of chain extender, polyol and blowing agent. Cell Polym 2009;28:145–58.
[29] Lefebvre J, Le Bras M, Bastin B, Paleja R, Delobel R. Flexible polyurethane foams: Flammability. J Fire Sci 2003;21:343–67.
[30] Thirumal M, Singha NK, Khastgir D, Manjunath BS, Naik YP. Halogen-free flame-retardant rigid polyurethane foams: effect of alumina trihydrate and triphenylphosphite on the properties of polyurethane foams. J Appl Polym Sci 2010;116:2260–8.
[31] Gómez-Fernández S, Ugarte L, Peña-Rodriguez C, Zubitur M, Corcuera MÁ, Eceiza A. Flexible polyurethane foam nanocomposites with modified layered double hydroxides. Appl Clay Sci 2016;123:109–20.
[32] Javni I, Song K, Lin J, Petrovic ZS. Structure and properties of flexible polyurethane foams with nano- and micro-fillers. J Cell Plast 2011;47:357–72.
[33] Gómez-Fernández S, Günther M, Schartel B, Corcuera MA, Eceiza A. Impact of the combined use of layered double hydroxides, lignin and phosphorous polyol on the fire behavior of flexible polyurethane foams. Ind Crop Prod 2018;125:346–59.
[34] Turner RB, Nichols JB, Kuklies RA. The influence of viscosity in cell opening of flexible molded foams. J Cell Plast 1989;25:117–24.
[35] Członka S, Strąkowska A, Kairytė A. Effect of walnut shells and silanized walnut shells on the mechanical and thermal properties of rigid polyurethane foams. Polym Test 2020;87:106534–48.
[36] Gayathri S, Jayabal P, Kottaisamy M, Ramakrishnan V. Synthesis of few layer graphene by direct exfoliation of graphite and a Raman spectroscopic study. AIP Adv 2014;4. 027116/12.
[37] Ferrari AC, Meyer JC, Scardaci V, Casiraghi C, Lazzeri M, Mauri F, et al. Raman spectrum of graphene and graphene layers. Phys Rev Lett 2006;97:1–4.
[38] Ferrari AC. Raman spectroscopy of graphene and graphite: disorder, electron-phonon coupling, doping and nonadiabatic effects. Solid State Commun 2007;143:47–57.
[39] Dresselhaus MS, Jorio A, Saito R. Characterizing graphene, graphite, and carbon nanotubes by Raman spectroscopy. Annu Rev Condens Matter Phys 2010;1:89–108.
[40] Khan U, O'Neill A, Lotya M, De S, Coleman JN. High-concentration solvent exfoliation of graphene. Small 2010;6:864–71.
[41] O'Neill A, Khan U, Nirmalraj PN, Boland J, Coleman JN. Graphene dispersion and exfoliation in low boiling point solvents. J Phys Chem C 2011;115:5422–8.
[42] Nemes-Incze P, Osváth Z, Kamarás K, Biró LP. Anomalies in thickness measurements of graphene and few layer graphite crystals by tapping mode atomic force microscopy. Carbon N Y 2008;46:1435–42.
[43] Zhou L, Fox L, Włodek M, Islas L, Slastanova A, Robles E, et al. Surface structure of few layer graphene. Carbon N Y 2018;136:255–61.
[44] Gupta S, Tai NH. Carbon materials as oil sorbents: a review on the synthesis and performance. J Mater Chem A 2016;4:1550–65.
[45] Cassie ABD, Baxter S. Wettability of porous surfaces. Trans Faraday Soc 1944:546–51.